Properties of obliquely propagating chorus

Olga P. Verkhoglyadova,[1,2] Bruce T. Tsurutani,[1] and Gurbax S. Lakhina[3]

Received 20 August 2009; revised 31 March 2010; accepted 27 May 2010; published 22 September 2010.

[1] We discuss chorus wave magnetic and electric field polarizations as functions on angle of propagation relative to the ambient magnetic field B_0. For the first time, it is shown using a cold plasma approximation that the general whistler wave has circularly polarized magnetic fields for oblique propagation. This theoretical result is verified by observations. The electric field polarization plane is not orthogonal to the wave vector k and is in general highly elliptically polarized. Both the magnetic and the electric polarizations have important consequences for cyclotron resonant electron pitch angle scattering and for electron energization, respectively. A special case of the whistler wave called the Gendrin mode is discussed.

Citation: Verkhoglyadova, O. P., B. T. Tsurutani, and G. S. Lakhina (2010), Properties of obliquely propagating chorus, *J. Geophys. Res.*, *115*, A00F19, doi:10.1029/2009JA014809.

1. Introduction

[2] Chorus is an electromagnetic wave in the whistler frequency range $\omega_{ci} < \omega < \omega_{ce}$ with unique sweeping frequency-time characteristics such that when played through a loudspeaker the emission sounds like birds chirping, hence the name. In the above, ω_{ci}, ω, and ω_{ce} are the ion cyclotron, wave, and electron cyclotron frequencies, respectively [*Krall and Trivelpiece*, 1973; *Stix*, 1992]. Chorus is observed in the outer region of the Earth's magnetosphere outside the plasmasphere [*Tsurutani and Smith*, 1974, 1977; *Anderson and Maeda*, 1977; *Koons and Roeder*, 1990; *Helliwell*, 1995; *Meredith et al.*, 2001, 2003a]. Because of presumed damping at $\omega = \omega_{ce}/2$, chorus is observed in two frequency bands, one above and one below the gap at $\omega \sim \omega_{ce}/2$ [*Tsurutani and Smith,* 1974]. In the Earth's nightside sector magnetosphere, chorus typically propagates almost parallel to the local background magnetic field B_0 ($\theta < 20°$), where θ is the angle between the wave vector k and B_0 [*Tsurutani and Smith*, 1977; *Tsurutani et al.*, 2009]. However, observations show that dayside chorus can also propagate at highly oblique angles [*Burton and Holzer*, 1974; *Goldstein and Tsurutani*, 1984] especially at midlatitudes to high latitudes. *Haque et al.* [2010] recently showed that both upper-band and lower-band chorus can propagate at low angles (~0°–20°) as well as at high angles (~50°–60°).

[3] It is the purpose of this paper to study the magnetic and electric polarization properties of chorus at all frequencies and at all angles of propagation. Although it is theoretically well known that whistler mode waves propagating parallel to B_0 are circularly polarized in both magnetic and electric field components [*Stix*, 1992], the properties of the waves for oblique angles of propagation are less well known. Even though general expressions for electromagnetic wave polarization in anisotropic plasma are derived in many textbooks, to our knowledge, a detailed analysis for oblique whistler wave mode is lacking. Knowledge of the polarization properties is critical for theoretical calculations of resonant wave-particle interactions. In this paper we use a theoretical (cold plasma) approach to identify the general whistler wave mode properties, with particular emphasis on the electric and magnetic field polarizations for obliquely propagating waves.

2. Wave Dispersion of the Whistler Mode

[4] We follow a general approach to study linear wave properties in a cold plasma approximation. Hereafter, we use the Gaussian (cgs) system of units and select a coordinate system such that B_0 is directed along the z axis and electromagnetic waves are assumed to propagate in the (xz) plane. These features are shown in Figure 1. For linear waves, all disturbances can be expressed by a series of plane waves with a single frequency (harmonics) of the Fourier transform, i.e., being proportional to $\exp[-i(\omega t - kr)]$, where k is the wave vector and r is the radius vector of the wavefront [*Landau and Lifshitz*, 1960]. Thus, the wave vector k in this geometry is $k = (k_\perp\ 0\ k_\parallel)$, where $k_\perp = k \sin\theta$, $k_\parallel = k \cos\theta$ are the perpendicular and parallel component of the wave vector k with respect to B_0.

[5] In these coordinates the Hermitian tensor of dielectric permittivity for cold magnetized plasma [*Krall and Trivelpiece*, 1973; *Sitenko and Malnev*, 1995] takes the form

$$\hat{\varepsilon} = \begin{pmatrix} \varepsilon_\perp & ig & 0 \\ -ig & \varepsilon_\perp & 0 \\ 0 & 0 & \varepsilon_\parallel \end{pmatrix}, \qquad (1)$$

[1]Jet Propulsion Laboratory, California Institute of Technology, Pasadena, California, USA.
[2]Center for Space Plasma and Aeronomic Research, University of Alabama in Huntsville, Huntsville, Alabama, USA.
[3]India Institute of Geomagnetism, Navi Mumbai, India.

0148-0227/10/2009JA014809

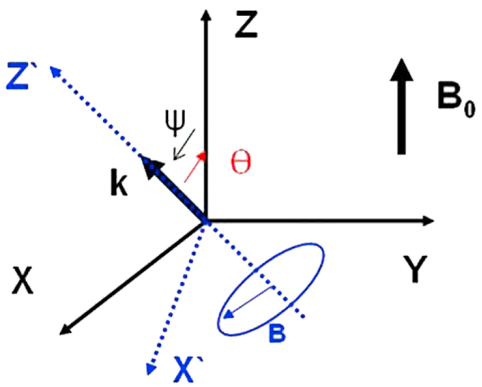

Figure 1. Wave geometry and coordinate systems used to study magnetic field polarization. The background magnetic field B_0 is directed along the z axis, and electromagnetic waves are assumed to propagate in the (xz) plane. Here k is the wave vector (see text for details).

where the components are defined by

$$\varepsilon_\perp \approx -\frac{\omega_{pe}^2}{\omega^2-\omega_{ce}^2}, \quad \varepsilon_\parallel \approx -\frac{\omega_{pe}^2}{\omega^2}, \quad g \approx -\frac{\omega_{pe}^2\,\omega_{ce}}{\omega\left(\omega^2-\omega_{ce}^2\right)}. \quad (2)$$

Here we have restricted the study to electron waves only and simplified the expressions in (2) by limiting the frequency range to $\omega_{ci} < \omega < \omega_{ce}$, and by assuming $\omega_{ce} < \omega_{pe}$, $\omega_{ce} < \omega_{pi}$. In the above, ω_{pi}, ω_{pe} are the ion and electron plasma frequencies.

[6] The general wave dispersion relation obtained with Maxwell equations [*Landau and Lifshitz*, 1960; *Krall and Trivelpiece*, 1973] is

$$\left(\frac{\omega^2}{c^2}\,\varepsilon_{ij} - k^2\,\delta_{ij} + k_i\,k_j\right) E_j = 0, \quad i,j = x,\,y,\,z, \quad (3)$$

where $\hat{\delta}$ is the unity tensor and E_j are the wave electric field components. This dispersion relation can be simplified for electromagnetic waves in the wave range of $\omega_{ci} \ll \omega \ll \omega_{ce}$:

$$\omega = \frac{\omega_{ce}\,c^2}{\omega_{pe}^2}\,\frac{k_\parallel k}{1+k^2a_e^2}, \quad a_e = \frac{c}{\omega_{pe}}, \quad (4)$$

where a_e is the electron inertial length.

[7] Assuming $k^2a_e^2 \ll 1$ in general equation (4), one derives the well-known dispersion relation under the standard approximation of the low-frequency whistler mode:

$$\omega = \omega_{ce}\,c^2\,k^2\,\cos\theta/\omega_{pe}^2. \quad (5)$$

Below we will discuss physical background used in the calculations. We will also justify why neither a nonlinear approach nor a hot plasma approach were necessary for the current study.

3. Theoretical Assumptions

[8] The theoretical approach used in this paper is based on Fourier transformation into harmonic components. Our results on the polarization properties of chorus are applicable for linear or small-amplitude plane waves. It is well known that chorus wave emission consists of separate "elements" rising or falling in frequency, which have fine structure of "wave packets" or "subelements." These features were extensively studied by *Santolik et al.* [2003, 2004], *Verkhoglyadova et al.* [2009], and *Tsurutani et al.* [2009]. Each subelement is a quasi-monochromatic wave modulated by a low-frequency signal. We assume that our linear approach is applicable within a single subelement for a quasi-periodic electromagnetic disturbance.

[9] Thermal effects can be neglected. The cold plasma model is valid under the condition of $(k\rho_e)^2 \ll 1$, where ρ_e is the electron gyroradius. For instance, $(k\rho_e)^2 \le 0.001$ if we assume a case of $k \le 1/a_e$ or $\lambda \ge 2\pi\,a_e \sim 20$ km. Here we used a smallness of the parameter $\left(\frac{\rho_e}{a_e}\right)^2 \ll 1$ for typical magnetospheric chorus conditions. The cold plasma model holds also for the waves having up to 10 times shorter wavelengths, i.e., $\lambda \ge 2$ km. In the paper we assume a frequency ratio, $\frac{\omega_{pe}}{\omega_{ce}} = 4.5$. This falls within the estimates by *Meredith et al.* [2003b] and *Horne et al.* [2003]. Under storm-time conditions, the frequency ratio ω_{pe}/ω_{ce} can be reduced from 4.5 to ~1.5 [*Horne et al.*, 2005], which further justifies the cold plasma model used.

[10] In this study we focus on electron effects only and exclude ion terms in components of the dielectric permittivity tensor for cold magnetized plasma (2). Thus, our results hold for waves with frequencies above certain limiting frequency range. For a sample chorus wave with $\omega \approx 0.2\ \omega_{ce}$ and typical magnetospheric $\frac{\omega_{pe}}{\omega_{ce}} = 4.5$, a ratio of ion to electron terms in $\varepsilon_\perp$ is 0.025, which is in accord with our approximations.

4. Polarization of the Whistler Mode

[11] The general wave polarization properties can be derived by using formulae (1–3). We find the following relationships between components E_j:

$$E_x = -i\,\frac{\omega^2 + \left(\omega^2-\omega_{ce}^2\right)k^2a_e^2}{\omega\,\omega_{ce}}\,E_y = i\,A_1\,E_y,$$
$$E_x = \frac{\omega_{pe}^2 + k_\perp^2c^2}{k_\perp\,k_\parallel c^2}\,E_z = A_2\,E_z, \quad (6)$$
$$A_1 = \frac{1+k^2a_e^2\sin^2\theta}{\cos\theta}, \qquad A_2 = \frac{1+k^2a_e^2\sin^2\theta}{k^2a_e^2\sin\theta\cos\theta}.$$

The wave "polarization" is often defined in terms of the electric field components, i.e., by (6) [see *Stix*, 1992]. However, we note that the magnetic component of electromagnetic waves is as important as the electric field component. It is the magnetic component of electromagnetic chorus waves that is responsible for cyclotron resonant pitch angle scattering of energetic electrons [*Tsurutani and Lakhina*, 1997]. The wave electric component is important for diffusive mechanism of particle energization [*Albert and Young*, 2005]. In this paper we will discuss the polarization of both electric and magnetic components. We will start with the magnetic components B_j below.

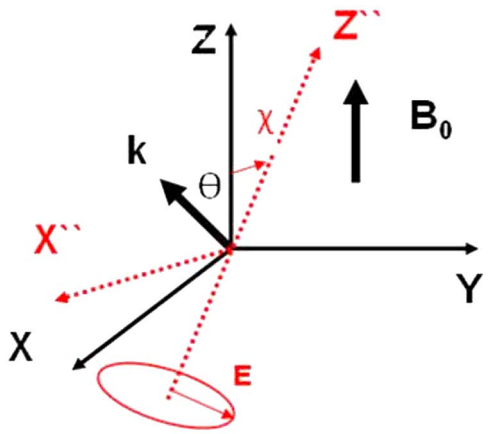

Figure 2. Wave geometry and coordinate systems used to study the electric field polarizations. The background magnetic field B_0 is directed along the z axis, and electromagnetic waves are assumed to propagate in the (xz) plane. Here k is the wave vector (see text for details).

[12] Using Maxwell equations $\nabla E = -\frac{1}{c}\frac{\partial B}{\partial t}$ and $\nabla B = 0$ and (6), it is easy to find the corresponding polarization relations for a plane wave:

$$B_x = -\frac{k_{||}}{k_\perp} B_z, \quad B_x = i\frac{k_{||}}{A_1\left(k_{||} - \frac{k_\perp}{A_2}\right)} B_y. \tag{7}$$

Below we consider several special cases of (7).

4.1. Parallel Propagation

[13] First, consider the simple case of a strictly parallel propagating electromagnetic whistler mode wave ($\theta = 0°$ and $k_\perp = 0$). Since equation (7) contains $k_\perp$ in denominator, we need to use the general relationships (3) and (2) to determine the polarization of the waves. In the case of parallel propagation, the general equation (3) splits into electromagnetic waves ($E_z = 0$) and electrostatic waves $E_z \neq 0$, $\varepsilon_{||} = 0$ [see *Sitenko and Malnev*, 1995]. We then use Maxwell's equations to transform the wave electric field into wave magnetic field. This is similar to the transformation of (6) into (7). For the electromagnetic wave branch, we obtain $E_x = iE_y$, $E_z = 0$, and $B_x = iB_y$, $B_z = 0$. Thus, parallel propagating electromagnetic whistler mode waves are circularly (right-hand) polarized in a plane orthogonal to the wave propagation direction (k).

4.2. Oblique Propagation

[14] For off-axis propagating electromagnetic whistler mode waves, we can simplify relationship (7) by explicitly introducing the angle θ and using the whistler dispersion equation (4) with (6). In this case,

$$B_x = -\frac{1}{\tan\theta} B_z, \quad B_x = i\,\cos\theta\, B_y. \tag{8}$$

To determine the polarization, we perform a linear transformation of the coordinate system (xyz) by rotating it through an angle ψ about y axis (see Figure 1). We search for a coordinate system ($x'yz'$) in which a particular wave mode will be circularly polarized. It is important to find if such coordinate system is unique. Following *Korn and Korn* [1961, equations 14.10–18b], we introduce a coordinate transformation of the wave magnetic field $B' = \hat{T}\,B$ with the matrix:

$$\hat{T} = \begin{pmatrix} a & 0 & b \\ 0 & 1 & 0 \\ -b & 0 & a \end{pmatrix}, \quad a = \cos\psi, \;\; b = \sin\psi \tag{9}$$

Assuming right-hand circular polarization of the wave in this new coordinate system and using (9), we obtain from (8):

$$\begin{aligned} B'_x = iB'_y &= aB_x + bB_z \\ B'_y &= B_y \\ B'_z = 0 &= -bB_x + aB_z \end{aligned} \tag{10}$$

The equations (10) with (8) are satisfied if $\psi = -\theta$, i.e., a rotation of the coordinate system anticlockwise from the direction of the background magnetic field. This is also the unique solution of (10) given $0 \leq |\psi| < 90°$. The z' axis of this new coordinate system coincides with the wave propagation direction (see Figure 1). Note that the polarization plane ($x'y$) is orthogonal to the wave vector ($\vec{k} \cdot \vec{B} = 0$), which is natural for an electromagnetic wave as discussed in the textbook by *Landau and Lifshitz* [1960]. The magnetic field polarization plane is shown schematically in Figure 1.

[15] It should be noted that this ($x'y$) plane is not the polarization plane for the wave electric field. The electric field has a different plane, which will be discussed below. From the wave geometry in Figure 2, we expect that we can find a polarization plane for the wave electric field by rotation about the y axis through a different angle χ. In this new coordinate system ($x''yz''$), wave electric field components are given by

$$\begin{aligned} E''_x &= cE_x + dE_z \\ E''_y &= E_y \\ E''_z = 0 &= -dE_x + cE_z \end{aligned}, \quad c = \cos\chi, \;\; d = \sin\chi. \tag{11}$$

After using (6) and performing simple transformations, we obtain

$$\begin{aligned} &\tan\chi = \frac{E_z}{E_x} = \frac{1}{A_2} = \frac{k^2 a_e^2 \sin\theta\cos\theta}{1 + k^2 a_e^2 \sin^2\theta}, \\ &E''_x = iA_1\left(c + \frac{d}{A_2}\right)E''_y = i\frac{\sin\theta}{\sin\chi}k^2 a_e^2 E''_y, \quad E''_z = 0. \end{aligned} \tag{12}$$

The wave electric field components are elliptically polarized in the direction orthogonal to the z'' axis. The polarization plane ($x''y$) is shown schematically in Figure 2. If we assume wave propagation at $\theta = 30°$ relative to B_0 and assuming (for example) $\omega/\omega_{ce} = 0.2$, the corresponding $\chi \approx 7°$ gives an ellipticity estimate: $\varepsilon_E = \frac{|E''_x|}{|E''_y|} \approx 0.2\frac{\sin\theta}{\sin\chi} \approx 1.1$. Thus, the wave electric field is almost circularly polarized within an accuracy of ~10%. For the oblique chorus propagating at $\theta = 50°$ relative to B_0 with $\omega/\omega_{ce} = 0.2$, the corresponding $\chi \approx 10°$ gives an ellipticity estimate of $\varepsilon_E \approx 2$. Thus, oblique chorus has highly elliptically polarized electric field.

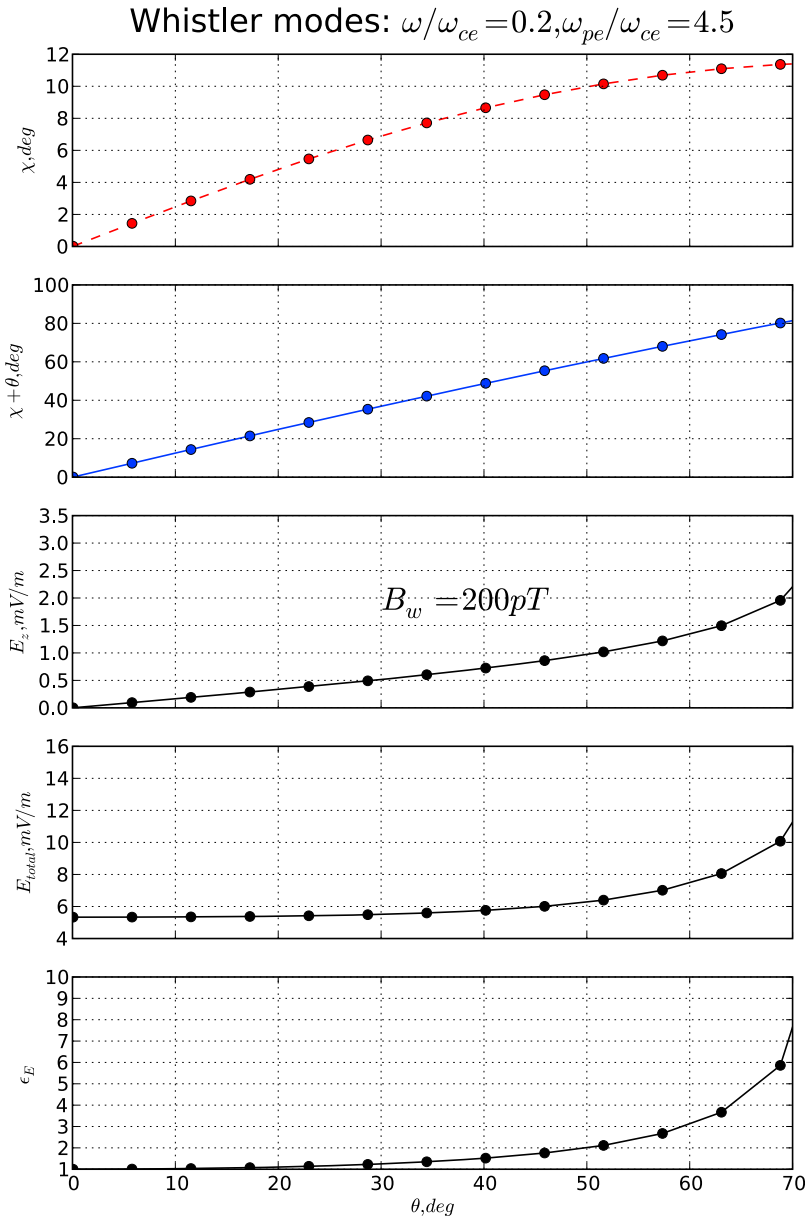

Figure 3. (a) Angle χ between the normal to the electric field polarization plane (k_E) and B_0, (b) angle $\chi + \theta$ between normal to the electric field polarization plane (k_E) and the wave propagation direction (k), (c) field-aligned wave electric field E_z, (d) total wave electric field, and (e) wave electric field ellipticity ε_E dependences on the chorus wave propagation angle (θ). Results are shown for a typical frequency ratio $\frac{\omega_{pe}}{\omega_{ce}} = 4.5$ and the frequency ratio $\frac{\omega}{\omega_{ce}} = 0.2$. A wave magnetic field amplitude of $B_w = 200$ pT is assumed for estimates in panels Figures 3c and 3d.

[16] We illustrate some of the wave properties for the case of whistler mode lower-band chorus waves with $\omega/\omega_{ce} = 0.2$ in Figure 3. Typical wave magnitude (B_w = 200 pT) and the frequency ratio are taken from Geotail measurements [*Tsurutani et al.*, 2009; *Verkhoglyadova et al.*, 2009]. Figures 3a and 3b show characteristic polarization plane angle dependences on the propagation angle θ. Figure 3e shows the wave ellipticity. For small angles of the wave propagation ($\theta < 30°$), the normal to the wave electric field polarization plane makes a small angle to B_0 (less than ~8°, Figure 3a). The ellipticity of the whistler wave electric field is small as well (Figure 3e). At the same time, Figure 3b shows that the angle between the normal to the electric field polarization plane and the wave propagation direction ($\theta + \chi$) can be quite large and is increasing for oblique whistlers (above ~30°). There is a substantial elliptical electric field polarization for oblique whistlers ($\varepsilon_E \geq 1.5$).

4.3. Wave Electric Field Magnitudes

[17] Whistler mode wave electric field measurements were recently discussed in studies by *Cattell et al.* [2008] and *Santolik* [2008]. From Maxwell's equations and using

the general dispersion equation (4), we can easily estimate the field-aligned electric field component ($|E_z|$) as well as the total electric field magnitude ($|E|$). These are given by the following expressions:

$$|E_z| = \frac{\omega_{ce}}{\omega_{pe}}|B_w|\frac{\sin\theta\cos\theta}{\sqrt{2}}\frac{k^3a_e^3}{1+k^2a_e^2},$$
$$|E| = \frac{\omega_{ce}}{\omega_{pe}}|B_w|\sqrt{\frac{2\cos^2\theta+\sin^2\theta\left(1+k^2a_e^2\right)^2}{2}}\frac{ka_e}{1+k^2a_e^2}. \quad (13)$$

We assume $\frac{\omega_{pe}}{\omega_{ce}} = 4.5$ as mentioned earlier. From Figures 3c and 3d, we find that the maximum electric field is ~6 mV/m for small angles of propagation. Corresponding value for E_z is ~0.5 mV/m up to 30°. Thus, we estimate whistler wave total electric field magnitudes between a few to tens of mV/m. Our theoretical estimates of chorus electric fields (based on assumed B_w and θ values) are in agreement with the observations of *Santolik* [2008]. Larger assumed B_w values will lead to larger E_z and |E| values, of course.

4.4. Gendrin Mode: A Special Case of Whistlers

[18] Some of chorus in the low-frequency band have been theoretically [*Gendrin*, 1961; *Dubinin et al.*, 2007], implicitly [*Lauben et al.*, 2002] and observationally [*Tsurutani et al.*, 2009; *Verkhoglyadova*, 2009; *Haque et al.*, 2010] noted to propagate at the so-called Gendrin angle. This angle θ_G is defined locally as $\cos\theta_G = 2\omega/\omega_{ce}$ and corresponds to the minimum value in wave refractive index parallel to the magnetic field line [*Gendrin*, 1961; *Dubinin et al.*, 2003]. The Gendrin angle can be quite large, ~50°–60° [*Verkhoglyadova et al.*, 2009]. The upper limit for the propagation angle θ is the resonance angle, $\cos\theta_r = \omega/\omega_{ce}$ [*Goldstein and Tsurutani*, 1984], which is larger than θ_G by definition and is typically above 70° for low-band ($\omega < \omega_{ce}/2$) chorus.

[19] On the basis of the general dispersion relation (4), we note that both the wave phase velocity (V_{ph}) and the component of the phase velocity along B_0 ($V_{ph||} = \omega/k_{||}$) attain maximum values at $k = 1/a_e$, and are given by

$$V_{ph||}^{max} = \frac{\omega_{ce}a_e}{2} = V_{g||}, \qquad V_{ph}^{max} = \frac{\omega_{ce}a_e\cos\theta}{2} \quad (14)$$

where $V_{g||} = \partial\omega/\partial k_{||}$ is the component of the group velocity along B_0. This particular whistler mode, the Gendrin mode [*Gendrin*, 1961] can be described as

$$\omega = \omega_G = \omega_{ce}\cos\theta_G/2, k = 1/a_e. \quad (15)$$

This mode exists only for $\omega < 0.5\omega_{ce}$ (the lower band range). It is clear from (15) that the Gendrin mode is nondispersive and the wave number k (or the wavelength) is a constant of the medium. Further, the group velocity perpendicular to B_0, i.e., $V_{g\perp} = \partial\omega/\partial k_\perp$, vanishes for the Gendrin mode, as can be verified from (4) and (15). Hence, the group velocity of the Gendrin mode is directed along B_0, and according to (14), it is equal to the maximum of the parallel phase velocity [see also *Helliwell*, 1995; *Lauben et al.*, 2002; *Dubinin et al.*, 2007].

[20] Below we discuss wave properties of Gendrin mode waves (15). From polarization study performed using the same coordinate transformation approach (see Figure 1) with $\psi = -\theta_G$, it follows that the magnetic component of the Gendrin mode is noted to be right-hand circularly polarized in a plane perpendicular to the wave propagation direction.

[21] The wave electric field is analyzed next. Following (12), we find a polarization plane for the wave electric field component that can be identified by the rotation angle $\chi > 0$ (see Figure 2):

$$\tan\chi = \frac{E_z}{E_x} = \frac{\sin\theta_G\cos\theta_G}{1+\sin^2\theta_G}, \quad E_x'' = i\frac{\sin\theta_G}{\sin\chi}E_y'', \quad E_z'' = 0. \quad (16)$$

From the above, it is noted that ellipticity of the wave electric field increases with increasing Gendrin angle.

[22] The maximum value of the angle $\chi_{max} = \arctan(1/\sqrt{8})$ is ~19.5° for $\theta_G{}^* = \arcsin(1/\sqrt{3}) \approx 35.3°$ and $\omega_G = \omega_{ce}/\sqrt{6} \approx 0.4\,\omega_{ce}$. It is interesting to note, that χ_{max} coincides with the value for a maximum of $(\alpha + \theta)$, where the angle α is between k and the "ray direction" or the group velocity direction [*Storey*, 1953]. This angular parameter defines ray "bunching" around the direction of B_0. For the Gendrin mode, the group velocity is aligned with B_0 and $\alpha = \theta_G$; thus, $\sin(2\theta_G{}^*) = 2\sin(\theta_G{}^*)\cos(\theta_G{}^*) = \sqrt{8}/3$ and $\alpha + \theta_G = 2\theta_G{}^* = \arctan(\sqrt{8})$. We obtain that $\tan(\alpha + \theta_G{}^*)\tan(\chi_{max}) = 1$ or $\chi_{max} = \pi/2 - 2\theta_G{}^*$.

[23] We estimate the Gendrin mode electric field by simplifying (13):

$$|E_z| = \frac{\omega_{ce}}{\omega_{pe}}|B_w|\frac{\sin\theta\cos\theta}{2\sqrt{2}}, \; |E| = \frac{\omega_{ce}}{2\omega_{pe}}|B_w|\sqrt{1+\sin^2\theta}. \quad (17)$$

For the case of $\theta_G = 56°$ [*Tsurutani et al.*, 2009], the corresponding angle χ is 15° and the ellipticity factor $\frac{\sin\theta_G}{\sin\chi}$ is about 3. Thus, electric fields for oblique Gendrin modes are highly elliptically polarized.

[24] The general results on Gendrin modes are summarized in Figure 4. Figures 4a and 4b are the angle χ between the normal to the electric field polarization plane and B_0 and the angle $\theta + \chi$ between the normal to the electric field polarization plane and the wave propagation direction. Figures 4c and 4d give the field-aligned electric field and the total electric field according to (17). Figure 4e shows the Gendrin mode frequency as a function of the Gendrin angle. Our estimate of the Gendrin mode electric field $|E_z|$ gives an upper limit of ~2.5 mV/m at $\theta_G = 45°$. The total electric field $|E|$ can reach ~9.5 mV/m for large propagation angles. It is noted that there is a lower limit of the Gendrin mode wave frequency (the lower hybrid frequency) and correspondingly an upper limit on the Gendrin angle.

5. Conclusions

5.1. Magnetic Components of Chorus Waves

[25] It has been theoretically demonstrated for the first time that the wave magnetic field for oblique electromagnetic waves of the whistler frequency range (4) is circularly polarized. This result was obtained in the cold plasma model. Thus, it is valid under the condition $(k\rho_e)^2 \ll 1$. The polarization is right handed, and the polarization plane is perpendicular to the wave propagation direction. It should be noted that all studies employing the minimum variance analysis (MVA) on magnetic data [*Smith and Tsurutani*, 1976] identify the plane perpendicular to the minimum

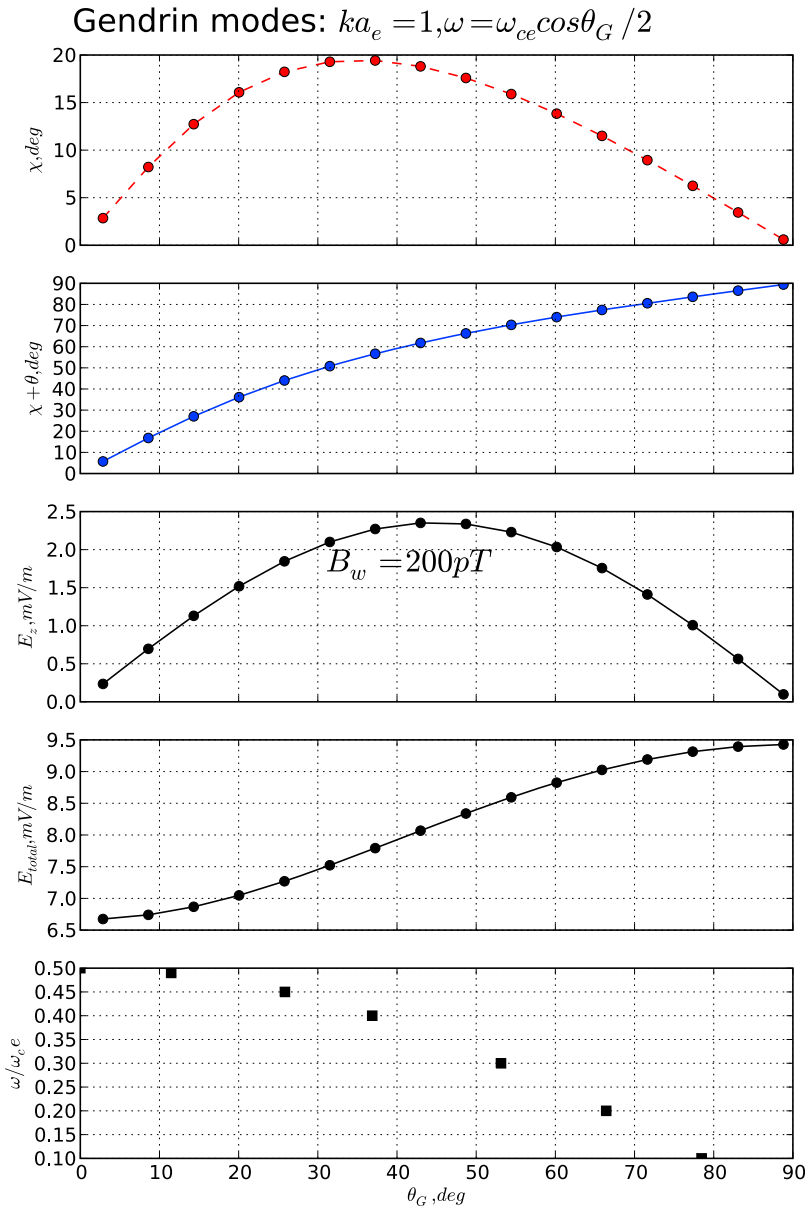

Figure 4. The Gendrin mode wave characteristics as functions of propagation angle (θ_G) for (a) angle χ between normal to the electric field polarization plane (k_E) and B_0, (b) angle $\chi + \theta$ between normal to the electric field polarization plane (k_E) and the wave propagation direction (k), (c) field-aligned electric field E_z, (d) total electric field E, (e) Gendrin mode frequencies ω_G. A wave magnetic field amplitude of B_w = 200 pT is assumed for estimates in panels Figures 4c and 4d. We use a typical frequency ratio of $\frac{\omega_{pe}}{\omega_{ce}} = 4.5$.

variance (i.e., wave propagation) direction for the wave polarization determination. Therefore, the MVA technique applied to chorus wave polarization should always give circular polarization for the magnetic component. This has been observed by *Goldstein and Tsurutani* [1984] for a considerable number of middle magnetospheric events and more recently by *Tsurutani et al.* [2009] for a limited number of dayside outer zone events.

5.2. Electric Component of Chorus Waves

[26] With the singular exception of a parallel propagating, circularly polarized wave, chorus electric fields are elliptically polarized. The ellipticity is small for quasi-parallel propagating waves and increases with increasing off-axis propagation. Electric fields for oblique whistler waves are highly elliptically polarized. An example was shown to illustrate a case with an ellipticity of ~3. The estimates of an angle $\theta + \chi$, between normal to the electric field polarization plane and the wave propagation direction, indicate that the polarization planes for the wave magnetic and electric fields are different, especially for obliquely propagating waves.

[27] **Acknowledgments.** Portions of this research were done at the Jet Propulsion Laboratory, California Institute of Technology under con-

tract with NASA. G.S.L. thanks the Indian National Science Academy, New Delhi, for support under the Senior Scientist Scheme.

[28] Zuyin Pu thanks the reviewers for their assistance in evaluating this paper.

References

Albert, J. M., and S. L. Young (2005), Multidimensional quasi-linear diffusion of radiation belt electrons, *Geophys. Res. Lett.*, *32*, L14110, doi:10.1029/2005GL023191.

Anderson, R. R., and K. Maeda (1977), VLF emissions associated with enhanced magnetospheric electrons, *J. Geophys. Res.*, *82*(1), 135–146, doi:10.1029/JA082i001p00135.

Burton, R. K., and R. E. Holzer (1974), The origin and propagation of chorus in the outer magnetosphere, *J. Geophys. Res.*, *79*(7), 1014–1023, doi:10.1029/JA079i007p01014.

Cattell, C., et al. (2008), Discovery of very large amplitude whistler-mode waves in Earth's radiation belts, *Geophys. Res. Lett.*, *35*, L01105, doi:10.1029/2007GL032009.

Dubinin, E., K. Sauer, and J. F. McKenzie (2003), Nonlinear stationary whistler waves and whistler solitons (oscillitons). Exact solutions, *J. Plasma Phys.*, *69*(4), 305–330.

Dubinin, E. M., et al. (2007), Coherent whistler emissions in the magnetosphere—Cluster observations, *Ann. Geophys.*, *25*, 303–315.

Gendrin, R. (1961), Le guidage des whistlers par le champ magnetique, *Planet. Space Sci.*, *5*, 274–278.

Goldstein, B. E., and B. T. Tsurutani (1984), Wave normal directions of chorus near the equatorial source region, *J. Geophys. Res.*, *89*(A5), 2789–2810, doi:10.1029/JA089iA05p02789.

Haque, N., M. Spasojevic, O. Santolik, and U. S. Inan (2010), Wave normal angles of magnetospheric chorus emissions observed on the Polar spacecraft, *J. Geophys. Res.*, *115*, A00F07, doi:10.1029/2009JA014717.

Helliwell, R. A. (1995), The role of the Gendrin mode of VLF propagation in the generation of magnetospheric emissions, *Geophys. Res. Lett.*, *22*(16), 2095–2098, doi:10.1029/95GL02003.

Horne, R. B., S. A. Glauert, and R. M. Thorne (2003), Resonant diffusion of radiation belt electrons by whistler-mode chorus, *Geophys. Res. Lett.*, *30*(9), 1493, doi:10.1029/2003GL016963.

Horne, R. B., et al. (2005), Wave acceleration of electrons in the Van Allen radiation belts, *Nature*, *437*, 227–230.

Koons, H. C., and J. L. Roeder (1990), A survey of equatorial magnetospheric wave activity between 5 and 8 R_E, *Planet. Space Sci.*, *38*(10), 1335–1341.

Korn, G. A., and T. M. Korn (1961), *Mathematical Handbook for Scientists and Engineers*, 2nd ed., McGraw-Hill, New York.

Krall, N. A., and A. W. Trivelpiece (1973), *Principles of Plasma Physics*, McGraw-Hill, New York.

Landau, L. D., and E. M. Lifshitz (1960), *Electrodynamics of Continuous Media*, vol. 8, *Course of Theoretical Physics*, Pergamon, Oxford.

Lauben, D. S., U. S. Inan, T. F. Bell, and D. A. Gurnett (2002), Source characteristics of ELF/VLF chorus, *J. Geophys. Res.*, *107*(A12), 1429, doi:10.1029/2000JA003019.

Meredith, N. P., R. B. Horne, and R. R. Anderson (2001), Substorm dependence of chorus amplitudes: Implications for the acceleration of electrons to relativistic energies, *J. Geophys. Res.*, *106*(A7), 13,165–13,178, doi:10.1029/2000JA900156.

Meredith, N. P., M. Cain, R. B. Horne, and D. Summers (2003a), Evidence for chorus-driven electron acceleration to relativistic energies from a survey of geomagnetically disturbed periods, *J. Geophys. Res.*, *108*(A6), 1248, doi:10.1029/2002JA009764.

Meredith, N. P., R. B. Horne, R. M. Thorne, and R. R. Anderson (2003b), Favored regions for chorus-driven electron acceleration to relativistic energies in the Earth's outer radiation belt, *Geophys. Res. Lett.*, *30*(16), 1871, doi:10.1029/2003GL017698.

Santolik, O. (2008), New results of investigations of whistler-mode chorus emissions, *Nonlinear Proc. Geophys.*, *15*, 621–630.

Santolik, O., D. A. Gurnett, J. S. Pickett, M. Parrot, and N. Cornilleau-Wehrlin (2003), Spatio-temporal structure of storm-time chorus, *J. Geophys. Res.*, *108*(A7), 1278, doi:10.1029/2002JA009791.

Santolik, O., D. A. Gurnett, J. S. Pickett, M. Parrot, and N. Cornilleau-Wehrlin (2004), A microscopic and nanoscopic view of storm-time chorus on 31 March 2001, *Geophys. Res. Lett.*, *31*, L02801, doi:10.1029/2003GL018757.

Sitenko, A., and V. Malnev (1995), *Plasma Physics Theory*, Chapman and Hall, London.

Smith, E. J., and B. T. Tsurutani (1976), Magnetosheath lion roars, *J. Geophys. Res.*, *81*(13), 2261–2266, doi:10.1029/JA081i013p02261.

Stix, T. (1992), *Waves in Plasmas*, AIP, New York.

Storey, L. R. O. (1953), An investigation of whistling atmospherics, *Philos. T. Roy. Soc. A, Math. Phys. Sci.*, *246*, 113–141.

Tsurutani, B. T., and G. S. Lakhina (1997), Some basic concepts of wave particle interactions in collisionless plasma, *Rev. Geophys.*, *35*(4), 491–501, doi:10.1029/97RG02200.

Tsurutani, B. T., and E. J. Smith (1974), Postmidnight chorus: A substorm phenomenon, *J. Geophys. Res.*, *79*(1), 118–127, doi:10.1029/JA079i001p00118.

Tsurutani, B. T., and E. J. Smith (1977), Two types of magnetospheric ELF chorus and their substorm dependencies, *J. Geophys. Res.*, *82*(32), 5112–5128, doi:10.1029/JA082i032p05112.

Tsurutani, B. T., O. P. Verkhoglyadova, G. Lakhina, and S. Yagitani (2009), Properties of dayside outer zone (DOZ) chorus during HILDCAA events: Loss of energetic electrons, *J. Geophys. Res.*, *114*, A03207, doi:10.1029/2008JA013353.

Verkhoglyadova, O. P., B. T. Tsurutani, Y. Omura, and S. Yagitani (2009), Properties of dayside nonlinear rising tone chorus emissions at large L observed by GEOTAIL, *Earth Planets Space*, *61*, 625–628.

G. S. Lakhina, India Institute of Geomagnetism, Navi Mumbai, Maharashtra 410 218, India.

B. T. Tsurutani and O. P. Verkhoglyadova, Jet Propulsion Laboratory, California Institute of Technology, Pasadena, CA 91109-8099, USA. (olga.verkhoglyadova@jpl.nasa.gov)